Optimized Design of Three-Dimensional Thermal Domes: A Comprehensive Approach

Junhao Gong[a,*]

School of Energy Science and Engineering, Harbin Institute of Technology, Harbin, 150001, China

junhao.gong@stu.hit.edu.cn

*Corresponding author

Keywords: thermal dome, Optimization Design, thermal metamaterial, transformation thermotics, thermal management, thermal invisibility

Abstract: This paper introduces the concept of a thermal dome, a novel thermal management strategy that overcomes the limitations of traditional thermal cloaks. The thermal dome is an open-structured device designed to manipulate heat conduction, effectively hiding target objects from thermal detection regardless of their heat-generating properties. The design approach involves mathematical methods to engineer the thermal dome with specific thermal conductivities that match the surrounding environment, thus maintaining the background temperature distribution and achieving thermal invisibility. The thermal dome's theoretical foundation is based on the Laplace equation, applicable to three-dimensional heat conduction scenarios. Verification of the thermal dome's functionality is conducted through finite-element simulations using COMSOL Multiphysics. The simulations demonstrate that the thermal dome can restore uniform temperature and isotherm distributions when an object with different thermal conductivity is introduced. The efficacy of the thermal dome is further analysed under different external temperature conditions, showing its robustness and adaptability. We also explore the thermal dome's performance under varying background thermal conductivities, utilizing effective medium theory to modify the dome's conductivity. The thermal dome presents a versatile and customizable solution for thermal management, with potential applications in military stealth, energy efficiency, and temperature monitoring.

1. Introduction

Heat conduction is the main form of heat transfer. In recent years, researchers have achieved many important achievements in the manipulation of heat conduction [1–3]. At the macroscale, researchers have designed various structures to achieve several functions, namely thermal cloak, thermal concentrator and thermal rotator [2,4–11]. At the microscale, based on phonon transport and scattering, devices like thermal transistor, thermal diode, thermal logic gates and thermal memory have become a reality [12–15]. Heat is also treated as an information carrier, which is utilized in communication, detection, anti-detection, and calculations [16–19]. To confront infrared detection, the concept of thermal invisibility has garnered significant attention due to its potential applications in various fields, such as military stealth, energy efficiency, and temperature monitoring [20,21].

Traditionally, thermal cloaks were designed by using thermally insulating materials to envelop the target, and then guiding the heat flow encompassment the cloaked region, thus achieving invisibility [16,21,22]. Various theories have been developed following this approach, such as transformation thermotics, scattering-cancellation, topology-optimization and machine learning [3,7–10,23–28]. Xu et.al designed a kind of bilayer cloak, which took geometrically anisotropic cases into consideration [22]. Ji et.al established an artificial network to design the properties of the thermal cloaks [25]. Sha et.al demonstrated topological functional cells (TFCs) to optimize thermal metamaterials traversing full-parameter anisotropic space [29]. Shen et.al experimentally fabricate a kind of thermal metamaterials, which can automatically change from a cloak (or concentrator) to a concentrator (or cloak) when the environmental temperature changes [11].

However, those cloaks have some inherent defects. Some of them require extreme properties, and

  DOI: 10.25236/icmmct.2024.020

most of the thermal cloaks fail to cope with different environments. In addition, they also base at closed and invariable structures, not allowing the existence of heat source. To address these challenges, we developed the novel concept known as the thermal dome. This concept deviates from the conventional cloaking methods by utilizing an open structure that not only allows for easy installation and convenient variation but also accommodates internal heat sources. The thermal dome is designed to manipulate heat conduction in a way that the target object is effectively hidden from thermal detection, regardless of its heat-generating capabilities.

This paper has proposed the mathematical methods to design the thermal dome. The thermal dome is engineered to exhibit specific thermal conductivities that match the surrounding environment. This match ensures that the temperature distribution within the background remains undisturbed, thereby achieving the goal of thermal invisibility. The design of the thermal dome is such that it can be reconfigured to adapt to different environmental conditions, making it a versatile solution for various engineering applications.

2. Theories of the thermal dome

We discuss heat transfer only by heat conduction in the three-dimensional case. In a homogeneous matrix with a constant thermal conductivity λ_b,heat flux would be distorted due to the introduction of an object with a different conductivity λ_a. To solve this problem, a thermal dome can be placed above the object, which recovers the temperature field outside and inside the dome. However, the dome can be designed in any form, we choose the hemispherical scheme. By changing the radii and thicknesses, domes can match various cases. Additionally, it also has excellent symmetry which simplifies the arithmetical operation. The heat transfer equation in the spherical coordinate system is written as

$$\rho c\frac{\partial T}{\partial t}=\frac{1}{r^2}\frac{\partial}{\partial r}\left(\lambda r^2\frac{\partial T}{\partial r}\right)+\frac{1}{r^2\sin^2\theta}\frac{\partial}{\partial \varphi}\left(\lambda\frac{\partial T}{\partial \varphi}\right)+\frac{1}{r^2\sin\theta}\frac{\partial}{\partial \theta}\left(\lambda\sin\theta\frac{\partial T}{\partial \theta}\right)+\dot{\phi}$$

where ρ, c, t, λ are the mass density, heat capacity, time and heat conductivity of the material, respectively. T denotes temperature and $\dot{\phi}$ denotes heat power density. It is presumed that the thermal conductivity is isotropic and all other thermal parameters, namely the mass density, specific heat capacity, and heat power density, are constants throughout the material. In the absence of heat sources, and under steady-state conditions where the temporal evolution of temperature is not considered, the governing equation for heat conduction within the material can be simplified to the Laplace equation:

$$\frac{1}{r^2}\frac{\partial}{\partial r}\left(r^2\frac{\partial T}{\partial r}\right)+\frac{1}{r^2\sin^2\theta}\frac{\partial}{\partial \varphi}\left(\frac{\partial T}{\partial \varphi}\right)+\frac{1}{r^2\sin\theta}\frac{\partial}{\partial \theta}\left(\sin\theta\frac{\partial T}{\partial \theta}\right)=0$$

In alignment with the preceding discourse, the thermal dome has been architected to exhibit exemplary performance across a multiplicity of operational contexts. To actualize this objective, a duo of essential prerequisites is posited: firstly, the whole surface upon which the foundation of the thermal dome is situated must be subject to uniform temperature regulation, ensuring a stable thermal boundary condition. Secondly, the interposition of an adiabatic layer between the dome and the core region is imperative, which serves to create a thermal barrier. The latter stipulation endows the thermal dome with the autonomy to function in isolation from the core region, irrespective of the conditions or contents therein.

By directly solving Laplace equation, the general solution of T can be written as

$$T_i=\sum_{m=0}^{\infty}\left[a_m^i r^m+b_m^i r^{-(m+1)}\right]P_m(\cos\theta)$$

where a_m^i and b_m^i $(i=1,2,3,4)$ are constants to be determined by the boundary conditions and T_i denotes the temperature in different regions: $i=1$ for the core region $(r<r_1), i=2$ for the

adiabatic layer ($r_1 < r < r_2$), $i = 3$ for the thermal dome ($r_2 < r < r_3$), $i = 4$ for the background ($r > r_3$). P_m is Legendre polynomial.

A uniform temperature gradient g is applied externally along the z direction. So when $r \to \infty$, T_4 tends to $gr\cos\theta$, which means $m = 1$ and $a_1^4 = g$. Considering in the ideal case, the temperature gradient is not distorted of the exterior region, so we set $b_1^4 = 0$ Additionally, when $r \to 0$, T_1 is limited, from which we can obtain $b_1^1 = 0$. Taking the continuities of temperature and heat flux into account, the boundary conditions can be written as

$$T_i|_{r=r_1,r_2,r_3} = T_{i+1}|_{r=r_1,r_2,r_3}$$

$$\lambda_i \frac{\partial T_i}{\partial r}|_{r=r_1,r_2,r_3} = \lambda_{i+1} \frac{\partial T_{i+1}}{\partial r}|_{r=r_1,r_2,r_3}$$

Therefore, the conductivity of the dome λ_d can be solved as

$$\lambda_d = \frac{2r_3^3 + r_2^3}{2(r_3^3 - r_2^3)}\lambda_b$$

3. Function verification and finite-element simulations

We use the commercial software COMSOL Multiphysics to do finite-element simulations and authenticate our theoretical analyses. We carried out steady-state simulations with the solid heat transfer module in three dimensions. The background is dimensioned at 40 × 40 × 20 cm^3 and its thermal conductivity λ_b is 15 W m^{-1} k^{-1}. An arbitrary object inside a hemispherical region with $r_1 = 10$ cm and thermal conductivity λ_0 = 400 W m^{-1} k^{-1} is introduced. The thicknesses of the adiabatic layer and thermal dome are 1 cm and 2 cm respectively and we obtain $r_2 = 12$ cm and $r_3 = 13$ cm. Therefore, we can set the conductivity of the dome λ_d as 98 W m^{-1} k^{-1}. The adiabatic layer features the conductivity $\lambda_a = 0.023$ W m^{-1} k^{-1}. The structure is shown in Fig.1. Next, we set the temperature of the top surface and bottom surface at 323 K and 273 K respectively and other faces of the background are all thermal adiabatic. We examine the efficacy of the thermal dome by comparing the temperature field in three distinct groups.

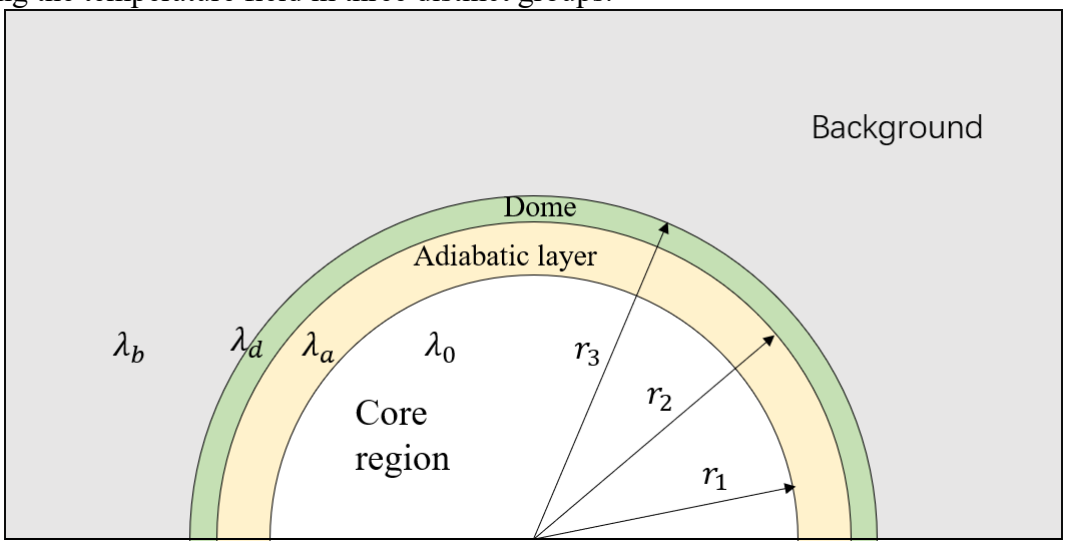

Figure 1: A schematic cross-sectional representation of the thermal dome.

As depicted in Fig.2, the temperature field and isotherm distributions are perturbed by the core region due to the difference between the core and the background. Obviously, after introducing the thermal dome, with an adiabatic layer, a uniform temperature and isotherm distributions reappear, precisely matching those of the pure background without the object. Due to the insulation caused by the adiabatic layer and the stabilization of the subface temperature, the temperature of core region keeps homogeneous and constant.

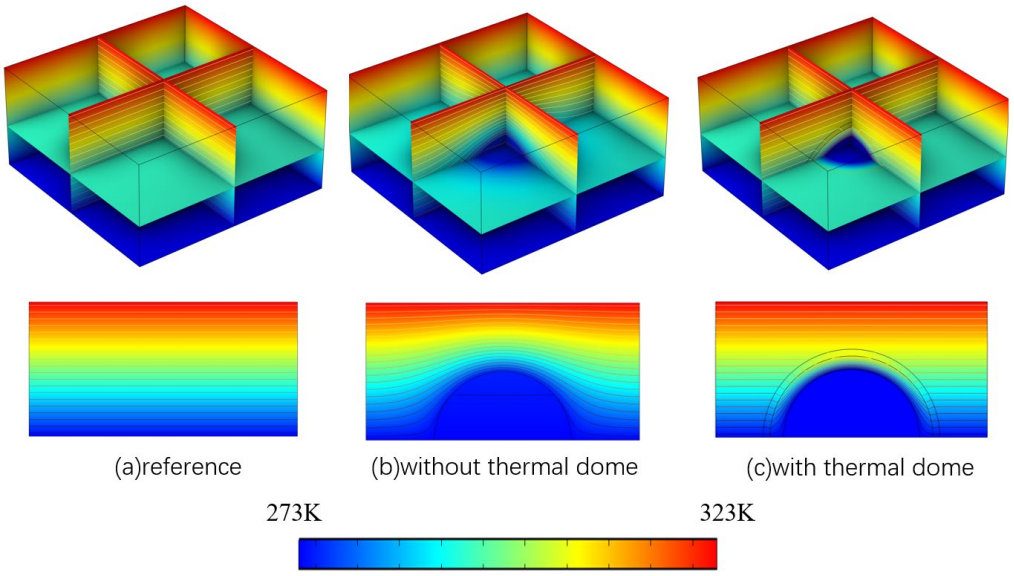

Figure 2: (a)-(c) The temperature distributions of the reference group, without a thermal dome and with a thermal dome, respectively.

For further quantitative analysis, the temperature data from a cross-section at $z = 8$ cm (-20 cm<y <20 cm) is imported. In order to directly reflect the temperature difference among the three groups, we define the dimensionless temperature $T^* = 100(T - T_0)/T_0$, where T_0 denotes the temperature of the reference group devoid of all the disturbance. As Fig.3 depicts, the group without thermal dome (green line) mismatches the reference obviously. In contrast, observing the group with dome (blue line), the values keep at 0 in the whole region outside the dome, confirming the powerful cloaking function of the thermal dome. No point on the green line is upon zero graduation line, which denotes the global influence of the introduction of the object.

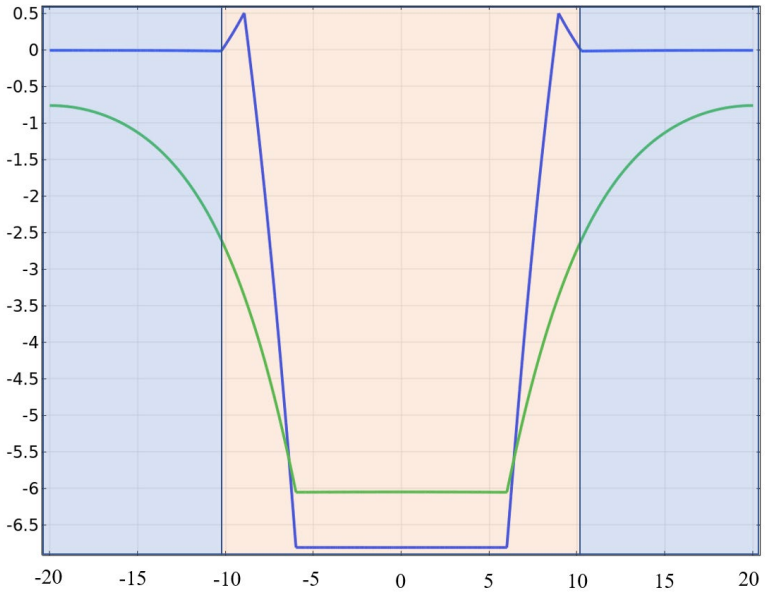

Figure 3: The graph of T^* varying with y coordinate. The green line denotes T^* of the group without a thermal dome and the blue line denotes T^* of the group with a thermal dome.

We also analyzed different external temperature conditions. The calculation method of λ_d is derived based on the case that the top and bottom surfaces of the cuboid which represents background are at constant higher and lower temperature respectively, while the other four vertical surfaces are thermal adiabatic. However, as depicted in Fig.4, the calculation method is also applicable in other cases. Fig.4(a) depicts that we apply a uniform temperature gradient along x direction instead of z direction. As shown in Fig.4(b) and Fig.4(c), the temperature field and isotherm distributions match

the reference group as well. Applying a uniform temperature gradient along y direction is in a similar way.

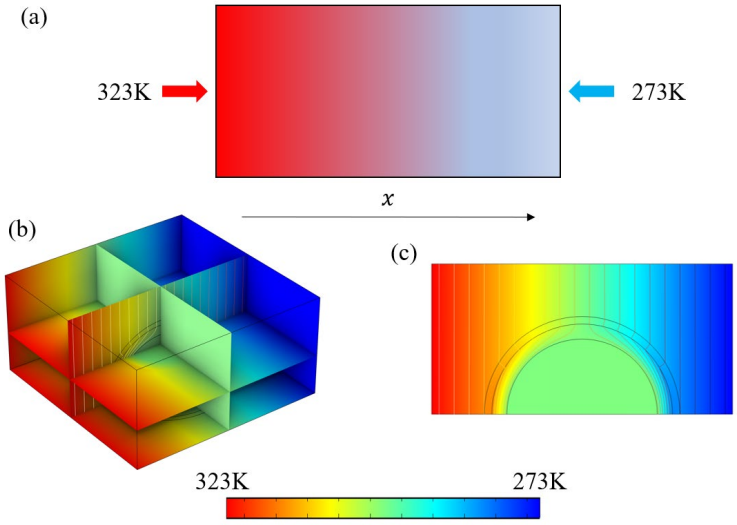

Figure 4: (a) The application of the uniform temperature gradient along x direction. (b) and (c) The efficacy of the thermal dome working in this different external temperature condition.

Thanks to the assumption that the whole subface is at constant temperature, we could take the heat source into consideration. We discuss the problem in two ways. Case 1: the heat capacity of the material from where the dome and core region are based is big enough, or there are some devices like heat reservoir inside the core region. These two conditions assure that the temperature of the subface can keep constant within a period of time, which means this kind of case is no difference between the case mentioned above. Case 2: the thermal diffusivity of the material from where the dome and core region are based is big enough, which assures the temperature of the whole subface increases at the same rate and the time scale of it is much smaller than the conduction process in the background. Under this condition, we can still handle this question as a steady statement problem.

Furthermore, the heat conductivity of the background is not always constant. To extend the applicable range of our thermal dome, we import effective medium theory as the theoretical foundation to modify the conductivity of the dome. The hemispherical shell structure of thermal domes makes it convenient to combine or split multilayer structures to obtain flexibly changed conductivities. As shown in Fig.5, we have proved the validity by simulating with and without the extra dome. We changed the parameter λ_0 from 15 W m^{-1} k^{-1} to 25 W m^{-1} k^{-1} and all the others stay constant. The conductivity of the newly added dome λ_d' is 80 W m^{-1} k^{-1} and its thickness is 1 cm, the same as the original dome (as depicted in Fig.5(a)). Fig.5(b) shows that the original dome loses its efficacy after the conductivity of the background has changed. By combining another thermal dome, obviously, the bilayer dome has rendered the temperature field back to normal.

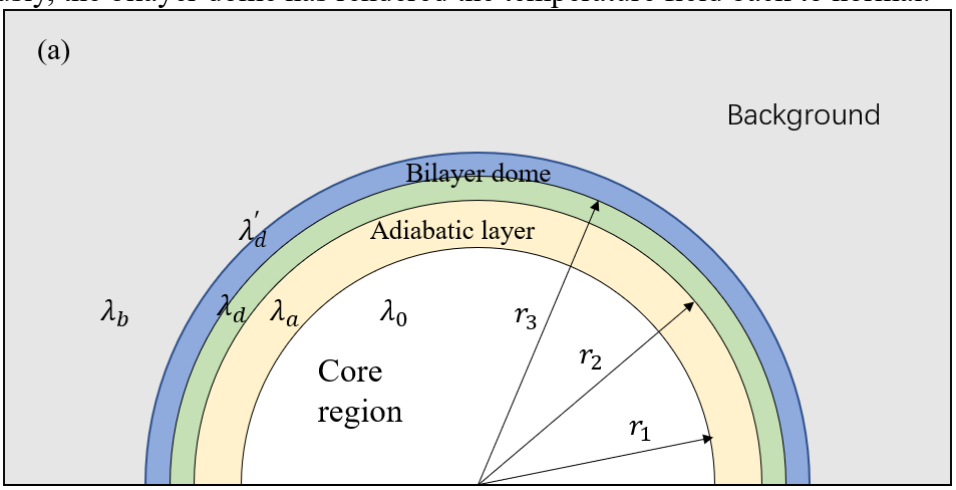

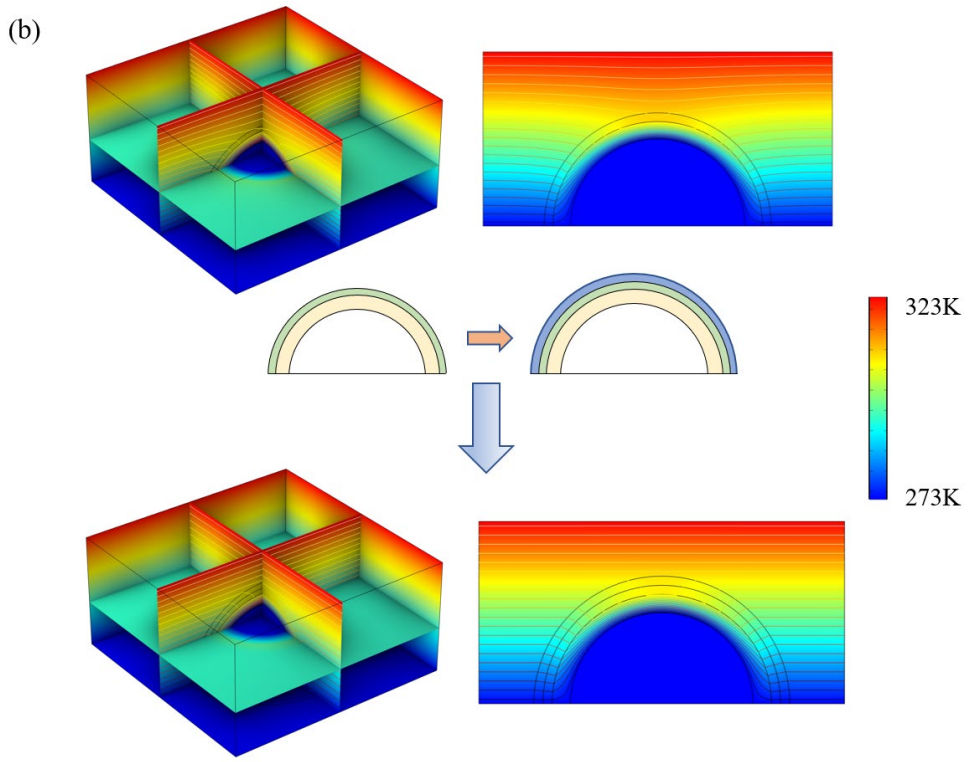

Figure 5: (a) The structure of the updated bilayer thermal dome. (b) When the background changes, the original dome could not realize the function of cloaking. After introducing reconfigured dome, the goal of cloaking is realized again.

4. Conclusions

In this paper, we proposed a new scheme of thermal dome, offering a novel thermal management strategy through the concept of it. By directly solving the Laplace equation, we obtain the general solutions of the temperature field. With boundary conditions, we finally derive the formula of the conductivity of the dome. Compared to the conventional thermal cloak, the thermal dome offers a more open and adaptable structure. The semispherical core region allows the existence of different objects inside and is not fully closed with the subface not covered. Additionally, the design of hemispherical shell is beneficial for combining and splitting multilayer-structure. As a result, in face of various background conditions (which means various thermal conductivities), this kind of thermal dome could fit perfectly. Users can customize a dome according to the specific circumstance.

Our numerical simulations by using Multiphysics COMSOL have demonstrated the efficacy of the thermal dome. Although we set the temperature of the whole subface as an isotherm boundary condition, we still discussed the feasibility in the realistic circumstance. With the help of thermal dome, we can easily control the heat conduction at will, achieving thermal invisibility.

The successful implementation of the thermal dome offers more optional thermal management strategies. One potential direction is to explore the thermal dome which works when heat conduction, convection and radiation concurred. Another possible direction is to explore the feasibility of different shapes of thermal domes, which could extend the sphere of application.

References

[1] C. Z. Fan, Y. Gao, and J. P. Huang, Shaped Graded Materials with an Apparent Negative Thermal Conductivity, Appl. Phys. Lett. 92, 251907 (2008).

[2] A. Greenleaf, Y. Kurylev, M. Lassas, and G. Uhlmann, Schrodinger's Hat: Electromagnetic, Acoustic and Quantum Amplifiers via Transformation Optics, Proc. Natl. Acad. Sci. 109, 10169 (2012).

[3] Y. Li, X. Shen, Z. Wu, J. Huang, Y. Chen, Y. Ni, and J. Huang, Temperature-Dependent Transformation Thermotics: From Switchable Thermal Cloaks to Macroscopic Thermal Diodes, Phys. Rev. Lett. 115, 195503 (2015).

[4] Y. Gao and J. P. Huang, Unconventional Thermal Cloak Hiding an Object Outside the Cloak, EPL Europhys. Lett. 104, 44001 (2013).

[5] J. Y. Li, Y. Gao, and J. P. Huang, A Bifunctional Cloak Using Transformation Media, J. Appl. Phys. 108, 074504 (2010).

[6] S. Narayana and Y. Sato, Heat Flux Manipulation with Engineered Thermal Materials, Phys. Rev. Lett. 108, 214303 (2012).

[7] T. Han, T. Yuan, B. Li, and C.-W. Qiu, Homogeneous Thermal Cloak with Constant Conductivity and Tunable Heat Localization, Sci. Rep. 3, 1593 (2013).

[8] T. Han, X. Bai, D. Gao, J. T. L. Thong, B. Li, and C.-W. Qiu, Experimental Demonstration of a Bilayer Thermal Cloak, Phys. Rev. Lett. 112, 054302 (2014).

[9] X. Y. Shen and J. P. Huang, Thermally Hiding an Object inside a Cloak with Feeling, Int. J. Heat Mass Transf. 78, 1 (2014).

[10] H. Xu, X. Shi, F. Gao, H. Sun, and B. Zhang, Ultrathin Three-Dimensional Thermal Cloak, Phys. Rev. Lett. 112, 054301 (2014).

[11] X. Shen, Y. Li, C. Jiang, Y. Ni, and J. Huang, Thermal Cloak-Concentrator, Appl. Phys. Lett. 109, 031907 (2016).

[12] B. L. Davis and M. I. Hussein, Nanophononic Metamaterial: Thermal Conductivity Reduction by Local Resonance, Phys. Rev. Lett. 112, 055505 (2014).

[13] J.-K. Yu, S. Mitrovic, D. Tham, J. Varghese, and J. R. Heath, Reduction of Thermal Conductivity in Phononic Nanomesh Structures, Nat. Nanotechnol. 5, 718 (2010).

[14] X. Shen, C. Jiang, Y. Li, and J. Huang, Thermal Metamaterial for Convergent Transfer of Conductive Heat with High Efficiency, Appl. Phys. Lett. 109, 201906 (2016).

[15] S. R. Sklan, X. Bai, B. Li, and X. Zhang, Detecting Thermal Cloaks via Transient Effects, Sci. Rep. 6, 32915 (2016).

[16] L. Xu and J. Huang, Metamaterials for Manipulating Thermal Radiation: Transparency, Cloak, and Expander, Phys. Rev. Appl. 12, 044048 (2019).

[17] G. Dai, J. Shang, and J. Huang, Theory of Transformation Thermal Convection for Creeping Flow in Porous Media: Cloaking, Concentrating, and Camouflage, Phys. Rev. E 97, 022129 (2018).

[18] F. Yang, B. Tian, L. Xu, and J. Huang, Experimental Demonstration of Thermal Chameleonlike Rotators with Transformation-Invariant Metamaterials, Phys. Rev. Appl. 14, 054024 (2020).

[19] Y. Peng, Y. Li, P. Cao, X. Zhu, and C. Qiu, 3D Printed Meta-Helmet for Wide-Angle Thermal Camouflages, Adv. Funct. Mater. 30, 2002061 (2020).

[20] R. Hu, S. Zhou, Y. Li, D. Lei, X. Luo, and C. Qiu, Illusion Thermotics, Adv. Mater. 30, 1707237 (2018).

[21] L. J. Xu, S. Yang, and J. P. Huang, Effectively Infinite Thermal Conductivity and Zero-Index Thermal Cloak, EPL Europhys. Lett. 131, 24002 (2020).

[22] L. Xu, J. Huang, T. Jiang, L. Zhang, and J. Huang, Thermally Invisible Sensors, Europhys. Lett. 132, 14002 (2020).

[23] R. Schittny, M. Kadic, S. Guenneau, and M. Wegener, Experiments on Transformation Thermodynamics: Molding the Flow of Heat, Phys. Rev. Lett. 110, 195901 (2013).

[24] Q. Ji, Y. Qi, C. Liu, S. Meng, J. Liang, M. Kadic, and G. Fang, Design of Thermal Cloaks with Isotropic Materials Based on Machine Learning, Int. J. Heat Mass Transf. 189, 122716 (2022).

[25] Q. Ji, X. Chen, J. Liang, G. Fang, V. Laude, T. Arepolage, S. Euphrasie, J. A. Iglesias Martínez, S. Guenneau, and M. Kadic, Deep Learning Based Design of Thermal Metadevices, Int. J. Heat Mass Transf. 196, 123149 (2022).

[26] W. Sha et al., Robustly Printable Freeform Thermal Metamaterials, Nat. Commun. 12, 7228 (2021).

[27] B. Peng, Y. Wei, Y. Qin, J. Dai, Y. Li, A. Liu, Y. Tian, L. Han, Y. Zheng, and P. Wen, Machine Learning-Enabled Constrained Multi-Objective Design of Architected Materials, Nat. Commun. 14, 6630 (2023).

[28] H. Chen, X. Tang, Z. Liu, Z. Liu, and H. Zhou, Predicting the Temperature Field of Thermal Cloaks in Homogeneous Isotropic Multilayer Materials Based on Deep Learning, Int. J. Heat Mass Transf. 219, 124849 (2024).

[29] W. Sha, R. Hu, M. Xiao, S. Chu, Z. Zhu, C.-W. Qiu, and L. Gao, Topology-Optimized Thermal Metamaterials Traversing Full-Parameter Anisotropic Space, Npj Comput. Mater. 8, 179 (2022).

1. 页面设置：

   (1)页边距：上：2.54cm，下：2.54cm，左：3.17cm，右：3.17cm

   (2)纸张：A4

   (3)版式：节的起始位置：接续本页，页眉：1.25cm，页脚：1.25cm，垂直对齐方式：顶端对齐

   (4)文档网格：无网格

2. 题目：Times New Roman，小二，加粗，左对齐，段前 24 磅，段后 18 磅。
3. 作者姓名：小四，加粗，左对齐，段后 12 磅。
4. 地址和邮编：10，两端对齐，斜体，无段前段后。
5. 关键词、摘要：10，两端对齐，段前 12 磅，段后 12 磅，Keywords, Abstract 后为“：”，并字体加粗，斜体。
6. 一级标题：10，加粗，两端对齐，段前 18 磅，段后 12 磅。编号使用样式为 1.,2.……，与下段同页，段中不分页。
7. 二级标题： 10，加粗，斜体，两端对齐，段前 12 磅，段后 12 磅。 编号使用样式为 1.1,1.2……，与下段同页，段中不分页。
8. 三级标题： 10，加粗， 斜体， 两端对齐，段前 6 磅，段后 6 磅。编号使用样式为 1.1.1,1.1.2……
9. 正文：10，首行缩进 0.5cm，段后 6 磅，单倍行距。
10. 参考文献：10，两端对齐，斜体。
11. 表头、图示：字号 10，居中，斜体，段前 6 磅，段后 6 磅。图片版式为嵌入型，无格式。表格对齐方式：居中，文字环绕：无。
12. 公式：右对齐，段前 6 磅。段后 6 磅。
13. 所列参考文献需要在文中标注引用